encit 2020

ABCM Associação Brasileira de Engenharia e Ciências Mecânicas

18th Brazilian Congress of Thermal Sciences and Engineering
November 16–20, 2020 (Online)

ENC-2020-0536
ANALYSIS AND SIMULATION OF THE CONJUGATE HEAT TRANSFER IN A MICROCHANNEL USING THE LATTICE BOLTZMANN METHOD

Ivan Talão Martins
Matheus dos Santos Guzella
Luben Cabezas Gómez
Engineering School of São Carlos - University of São Paulo
ivanmartins@usp.br, matheusguzella@gmail.com and lubencg@sc.usp.br

Abstract. *In this paper, a study of the Lattice Boltzmann method (LBM) is developed by solving a conjugate heat transfer problem in a microchannel. The convergence of the method is evaluated by comparing simulation results for different lattice sizes. Then, to evaluate the accuracy of the method, the numerical results are compared with a solution given by the commercial CFD software COMSOL®. The numerical results comprehend both, two and three dimensional simulation results. In order to validate the two dimensional simulation approach, results for the central longitudinal plane of the three dimensional domain will be used for checking the previous 2D results.*

Keywords: *Lattice Boltzmann method, conjugate heat transfer problem, boundary conditions for 2D LBM, microchannel simulation*

1. INTRODUCTION

Since the second half of the XIX century, the classical laws have been questioned with the discovery of the molecular, atomic and subatomic world, appearing new concepts and laws that would become a new approach to the study of Thermodynamics: the Statistical Thermodynamics. Then, with this new way to see the phenomena, new mathematical models were developed, such as the Boltzmann transport equation, which describes in a statistical way the behavior of system of particles. Hence, new methods to solve important transport problems such as heat conduction and fluid flow were able to be elaborated.

According to Krüger *et al.* (2017), it is possible to categorize the thermal-fluid simulation methods into three principals groups: the macroscopic, the mesoscopic and the microscopic methods. While the first use numerical methods to solve the discrete equations, such as Navier-Stokes equation, the second and the third are based in a mathematics that describes the material molecular and sub molecular iterations.

In general, the mesoscopic method have received more attention in the second half of the XX century, when Hardy *et al.* (1973) developed a simple 2D model to describe the behavior of gases, named HPP model. This model was based in square lattices, where the particles reside. The collision of these particles and after, the streaming between these lattices simulate the system behavior. Three years after, Hardy *et al.* (1976) proposed a model that allowed the simulation of fluids, namely the FHP method. The Lattice Boltzmann Method emerged from these lattice gas methods, from the substitution of the boolean variable to a particle distribution function in order to reduce the statistical noise.

In the literature, some studies investigate the conjugate heat transfer problem using the Lattice Boltzmann Method. For example, Tarokh *et al.* (2013), performed numerical simulations considering multiple heated obstacles mounted in a walled parallel-plate channel. The effects of the thermophysical and geometrical parameter on the local Nusselt number were investigated. The authors found that increasing the obstacle fluid thermal conductivity ratio and decreasing wall-to-obstacle thermal conductivity ratio results in increasing the local Nusselt number around the obstacle's periphery. However, this study was performed considering only two-dimensional simulations, which may limit the extension of the influence of the geometrical results in the Z direction. This fact was also pointed in the work of Yu *et al.* (2018).

Imani *et al.* (2012) studied the conjugate heat transfer considering multiple heated obstacles mounted in a walled parallel plate channel. The main objective of the authors was quite the same as the one from Tarokh *et al.* (2013). The main conclusion addressed by the authors was that increasing the obstacle-to-fluid thermal conductivity ratio results in increasing the local Nusselt number around the obstacle's periphery. On the other hand, the opposite was noticed when considering the effect of the wall-to-obstacle thermal conductivity ratio on the local Nusselt number. It should be stressed that the simulations were also performed in two dimensions.

Regarding the Lattice Boltzmann Method, the main advantage of this method is the ease of the numerical implementation, when it is compared with others method (e.g the finite element method, the finite volume method, etc). Also, due to its kinetic nature, the boundary conditions are also easily to implement, even for complex domains, such as a porous interface. Using this method, this paper puts forward numerical simulations of the conjugate heat transfer in a microchannel. Different from the previously mentioned papers, both two-dimensional and three-dimensional simulations are performed in the present work.

2. MATHEMATICAL MODEL

2.1 The Boltzmann Equation

The most important quantity in the Lattice Boltzmann Method is the particle distribution function f, which represents the density in a microscopic scale and it is a three-dimensional function of both coordinates and velocity spaces (Krüger *et al.*, 2017). Thus, based on the Boltzmann transport equation (Eq. (1)), to describe the mathematical behavior of the distribution function, there are two principals processes involved: the collision and the posterior streaming of f. The first can be represented by the collision operator Ω, which represent the inter-molecular force effects during the collision process. With respect to the second, it can be related with the left hand side of this equation, which, in essence, it is just an advection equation for f. It is important to know that, in Eq. (1), r is the directional index that could be x, y or z in a three-dimensional case and F/ρ are the specific forces acting in the domain.

$$\partial_t f + c \cdot \partial_r f + \frac{F}{\rho} \cdot \partial_c f = \Omega \tag{1}$$

In this way, following the book of Krüger *et al.* (2017), it is possible to calculate the macroscopic quantities using the conservation laws. These laws are represented in Eq. (2) and Eq. (3), in which **u** is the macroscopic velocity and **c** is the particle velocity, associated with the distribution function.

$$\int f(\mathbf{x}, \mathbf{c}, t)\, d^3c = \rho(\mathbf{x}, t) \tag{2}$$

$$\int \mathbf{c} f(\mathbf{x}, \mathbf{c}, t)\, d^3c = \rho \mathbf{u}(\mathbf{x}, t) \tag{3}$$

2.2 The Lattice Boltzmann Method

The Boltzmann equation represents an advection equation. However, the collision operator is complicated and difficult to handle. In this sense, regarding the collision operator, Bhatnagar, Gross, and Krook proposed a very simple approximation in 1954, namely the BGK operator, which can be seen in Eq. (4), in which τ is the relaxation parameter.

$$\Omega = \frac{1}{\tau} \cdot (f^{eq} - f) \tag{4}$$

The discretization of Eq. (1) is performed in the velocity space and, considering that there is no force acting in the domain. Later, the space and time discretizations are also performed and the Lattice Boltzmann Equation can be obtained, as shown in Eq. (5):

$$f_i(\mathbf{x} + \mathbf{c_i} \cdot \Delta t, t + \Delta t) - f_i(\mathbf{x}, t) = \frac{\Delta t}{\tau} \cdot [f_i^{eq}(\mathbf{x}, t) - f_i(\mathbf{x}, t)] \tag{5}$$

The discretization in the velocity space is followed by a specific choice of the velocity scheme (also known as lattice arrangement). Some of these lattice arrangements for a two dimensional study are shown in Fig. 1:

Moreover, it is necessary to obtain the equilibrium distribution function (f_{eq}), which describes the particle distribution at the equilibrium condition. The particles assume an equilibrium stage where they are isotropic in the velocity space, i.e. $\mathbf{u} = \mathbf{c}$. This function is given by Eq. (6), in which w_i are the weights related with the velocities, which, for 1D and 2D cases, are given in the Fig. 2.

$$f_i^{eq} = w_i \cdot \rho \left(1 + \frac{\mathbf{c}_i \cdot \mathbf{u}}{c_s^2} + \frac{(\mathbf{c}_i \cdot \mathbf{u})^2}{2c_s^4} - \frac{\mathbf{u} \cdot \mathbf{u}}{2c_s^2} \right) \tag{6}$$

In addition, to obtain the macroscopic variables according to the conservation laws, the summation process of the discrete distribution function and its respective moments are performed, as shown in Eq. (7) and Eq. (8). However, to ensure the solution of an specific problem, there is a relation between the relaxation parameter and the macroscopic characteristics. For the mass and linear momentum conservation equations, this coupling is associated with the viscosity,

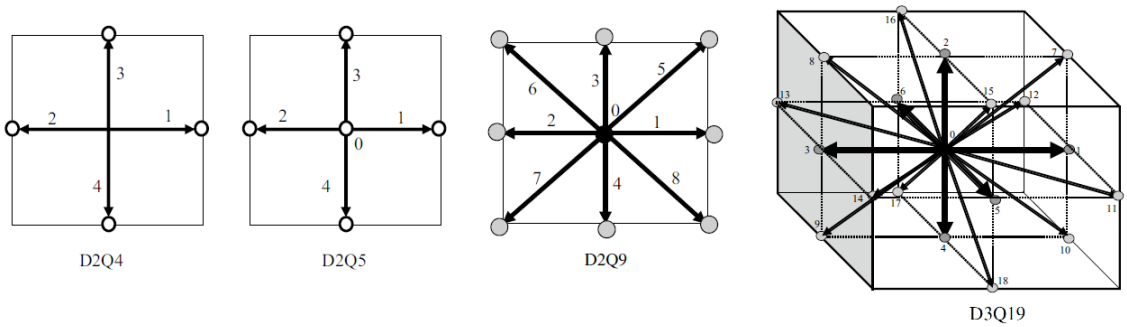

Figure 1. Lattice arrangements for 2D and 3D fields. Modified from: Mohamad (2019).

Model	Lattice vector $\boldsymbol{c}_i$	Weight w_i	c_s^2
D1Q3	0, ±1	2/3, 1/6	1/3
D1Q5	0, ±1, ±2	6/12, 2/12, 1/12	1
D2Q7	(0,0), $(\pm 1/2, \pm\sqrt{3}/2)$	1/2, 1/12	1/4
D2Q9	(0,0), (±1,0),(0, ±1), (±1, ±1)	4/9, 1/9, 1/36	1/3
D3Q15	(0,0,0), (±1,0,0), (0, ±1,0),(0,0, ±1), (±1, ±1, ±1)	2/9, 1/9, 1/72	1/3
D3Q19	(0,0,0), (±1,0,0), (0, ±1,0),(0,0, ±1), (±1, ±1,0), (±1,0, ±1),(0, ±1, ±1)	1/3, 1/18, 1/36	1/3

Figure 2. Values of weights, velocities and sound velocity for 1D and 2D velocity schemes (lattice arrangements. Available from: Guo and Shu (2013).

being the relation between the macroscopic and mesoscopic scales identified by Eq. (9). In this equation c_s, represents the sound speed, which is a constant value for a specified velocity scheme.

$$\sum_i f_i(\mathbf{x}, t) = \rho(\mathbf{x}, t) \tag{7}$$

$$\sum_i \mathbf{c_i} f_i(\mathbf{x}, t) = \rho \cdot \mathbf{u}(\mathbf{x}, t) \tag{8}$$

$$\tau = \frac{\nu \cdot \Delta t}{c_s^2 \cdot \Delta x^2} + 0.5 \tag{9}$$

Even though it becomes possible to calculate the distribution function collisions, there are still unknown operations, such as the streaming and the boundary conditions. Thus, considering the streaming, this operation becomes simple to evaluate, because of the velocity discretization. In this way, it consists of only move the functions between the lattices according to each direction, such as the Eq. (11) indicates. That is one of the reasons that the Lattice Boltzmann Method is characterized to be simpler to implement than other methods, such as the Finite Element Method, for example.

$$f_i^*(\mathbf{x}, t) = f_i(\mathbf{x}, t) + \frac{\Delta t}{\tau} \cdot [f_i^{eq}(\mathbf{x}, t) - f_i(\mathbf{x}, t)] \tag{10}$$

$$f_i(\mathbf{x} + \mathbf{c_i} \cdot \Delta t, t + \Delta t) = f_i^*(\mathbf{x}, t) \tag{11}$$

Besides that, likewise the macroscopic variables related with the movement of fluids are calculated, it is possible to assume a temperature distribution function g_i, which represents the conservation of energy by an equation for computing a particular scalar C, that represents the temperature of the fluid or solid domain (Krüger *et al.*, 2017). Therefore, the equilibrium distribution function for g_i consists in the Eq 12, in which the values related with fluid variable (e.q. velocity and density) must be computed before the populations of this thermal scalar parameter, the temperature.

$$g_i^{eq} = w_i \cdot C \left(1 + \frac{\mathbf{c}_i \cdot \mathbf{u}}{c_s^2} + \frac{(\mathbf{c}_i \cdot \mathbf{u})^2}{2c_s^4} - \frac{\mathbf{u} \cdot \mathbf{u}}{2c_s^2}\right) \tag{12}$$

Considering a conjugated heat transfer problem, it is required to evaluate first the values of the fluid variables. After doing this, as well as is performed with the distribution function f, the collision and the streaming of g_i has to be evaluate. Then, to obtain the macroscopic temperature C, a sum of all the functions in each lattice has to be done as indicate the Eq. (13).

$$\sum_i g_i(\mathbf{x}, t) = C(\mathbf{x}, t) \tag{13}$$

It is evident that is needed to relate the relaxation parameter τ_g with the thermal characteristics of the material in question. Then, as well as for the fluid viscosity, it is possible to relate the thermal fluid characteristics with this parameter by the Eq. (14), being α the thermal diffusion coefficient of the fluid or solid domain.

$$\tau_g = \frac{\alpha \cdot \Delta t}{c_s^2 \cdot \Delta x^2} + 0.5 \tag{14}$$

Moreover, it is important to note that, because of working with non-dimensional values in the simulations and considering the D2Q9 model, the Eq. (14) becomes $\tau_g = 3\alpha + 0.5$, such as Darzi *et al.* (2013) and Tarokh *et al.* (2013) showed respectively in each work. The same equations are obtained for the three-dimensional simulation, in which the D3Q19 are applied.

2.3 Boundary Conditions

2.3.1 Hydrodynamic boundary conditions

In order to close the numerical model, the next step consists in evaluating the boundary conditions. It should be stressed that only the equations for the D2Q9 are presented. For the velocity scheme D3Q19, the set of equations can be found, for example, in Hecht and Harting (2010).

In general, for stationary walls, one way to compute the unknown distribution functions is using the Bounce-Back method, which is based in the reflection of the populations, i.e., the function that is in the direction of the wall is bounced back and assumes the direction of the opposite function. Mathematically, this can be represented by the Eq. (15), in which $\bar{i}$ represents the direction opposite of the function i. For example, if f_i has the velocity c_i, $f_{\bar{i}}$ is in the same direction, but its velocity is $-c_i$.

$$f_{\bar{i}}(\mathbf{x_b}, t + \Delta t) = f_i^*(\mathbf{x_b}, t) \tag{15}$$

Similarly, for the inlet it is possible to use the non-equilibrium Bounce-Back condition. This rule consists in the computation of the unknown populations by the reflection of the non-equilibrium distribution function (f_i^{neq}), which is defined as the difference between the function and the equilibrium function. According to Krüger *et al.* (2017), basing in Eq. (15), knowing that $f_i^{neq} = f_i - f_i^{eq}$, with the equations of mass and momentum conservation and making use of the Eq. (6) to evaluate f_i^{eq}, it is possible to obtain the Eq. (16). This equation gives the density for an inlet boundary in the right side of the domain, but just for the D2Q9 arrangement. Then, being $u_{x,b}$ the inlet velocity (that is only in x direction), the unknown values of the functions at this boundary are in the Eq. (17).

$$\rho_b = \frac{1}{1 - u_{x,b}}[f_0 + f_2 + f_4 + 2(f_3 + f_6 + f_7)] \tag{16}$$

$$f_1 = f_3 + \frac{2}{3}\rho_b u_{x,b}; \qquad f_5 = f_7 - \frac{1}{2}(f_2 - f_4) - \frac{1}{6}\rho_b u_{x,b}; \qquad f_8 = f_6 + \frac{1}{2}(f_2 - f_4) + \frac{1}{6}\rho_b u_{x,b} \tag{17}$$

For the outlet, it is assumed that there, the pressure is equal to atmospheric. Thus, in the same way that Ho *et al.* (2009) has presented in his work, to evaluate this condition, it is possible to do the same procedure as to the inlet condition, but now with a density known. It is important to effort that, to get the density at the outlet boundary, the relation $p = \rho c_s^2$, with c_s being the sound speed (see Fig. 1). In this way, the conditions can be seen in Eq. 18.

$$f_3 = f_1 - \frac{2}{3}\rho_b u_{x,b}; \qquad f_7 = f_5 + \frac{1}{2}(f_2 - f_4) - \frac{1}{6}\rho_b u_{x,b}; \qquad f_6 = f_8 - \frac{1}{2}(f_2 - f_4) - \frac{1}{6}\rho_b u_{x,b} \tag{18}$$

However, to evaluate the unknown velocity, it is necessary to consider Eq. 19, that uses the value of known functions at boundary and of the density in the outlet.

$$u_{x,b} = \frac{1}{\rho_b}[f_0 + f_2 + f_4 + 2(f_1 + f_5 + f_8)] - 1 \tag{19}$$

2.3.2 Thermal boundary conditions

In the case of the thermal model, for the walls which are given a fixed temperature (i.e. Dirichlet boundary), the non-equilibrium bounce-back can be applied. Then, by Eq. (12) and Eq. (13), through algebraic manipulations it is possible to achieve the Eq. (20), in which w_i and $w_{\bar{i}}$ are the weights related with the distribution function used to solve the energy equation and T_b, the temperature at this limit.

$$g_{\bar{i}}(\mathbf{x_b}, t + \Delta t) = (w_i + w_{\bar{i}})T_b - g_i^*(\mathbf{x_b}, t) \tag{20}$$

In addition, for a constant heat flux boundary condition, according to Zhang *et al.* (2012), it is possible to transform a Neumann into a Dirichlet boundary condition. From Fourier's law at the normal direction of the boundary ($\mathbf{n}$): $\dot{q} = -k\partial_n T$, where k is the thermal conductivity of the material and $\dot{q}$, the flux at the wall. Thus, using the finite difference approach, it is possible to obtain the values of the wall temperature, as follows:

$$T_w = T_b + \frac{q|\mathbf{x_w} - \mathbf{x_b}|}{k} \tag{21}$$

Where $\mathbf{x_b}$ is the boundary node and $\mathbf{x_w}$ the solid node at the wall. Using the half-way approach for this boundary condition, the term $|\mathbf{x_w} - \mathbf{x_b}|$ can be expressed as $0.5\Delta x$. So, the Neumann flux condition has transformed in a Dirichlet temperature condition, which can be implemented as mentioned previously.

In the case of the outflow and the adiabatic walls, the heat flux is considered zero. In this case, is possible to use the bounce-back rule just like for the hydrodynamic distribution function.

The simulation steps are performed as follows: after the initialization of the variables, the computational operations inside the computational procedure start with the initialization of the particle distribution function, using the equilibrium form. Then, the collision calculation is performed. After that, the streaming process is carried and the calculation of boundary conditions and, finally the the macroscopic quantities calculation finishes the algorithm. It is important to state that the described procedure is performed first for the fluid flow and then for the temperature field.

3. CASE STUDY

In this paper, a microchannel is studied using the Lattice Boltzmann Method, considering a conjugate heat transfer problem. First, a two dimensional domain is analyzed, which is represented by Fig. 3. This domain represents a longitudinal cut in the middle section of the original channel. The dimensions of this 2D channel are $10mm$ of length and $200\mu m$ of height, and for the solid region, it has the same length, but $100\mu m$ of height. The upper wall and the solid side parts are considered perfectly insulated. For the lower wall, a $1000W/m^2$ heat flux is applied in the normal direction. The fluid in question is water, which enters into the channel at $T_0 = 20°C$, with a viscosity equal to $9.684 \cdot 10^{-7}m^2/s$ and a thermal diffusivity, $1.41 \cdot 10^{-7}m^2/s$. In addition, the solid part was considered to be silicon, with a thermal diffusivity equal to $9.307 \cdot 10^{-5}m^2/s$ and a thermal conductivity of $152.6W/mK$.

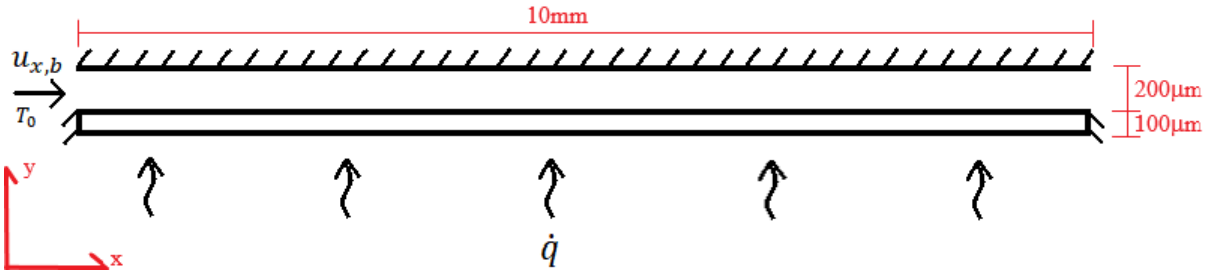

Figure 3. Two-dimensional representation of the microchannel.

The principal addressed problem is the calculation of flow and temperature fields along the microchannel length. At the same time that the number of lattices in y direction must not be very small to guarantee a good accuracy, the use of a high number can lead to a time consuming simulations due to the need of using a very large number of lattices in the x direction. This occurs because of the proportion of the domain dimensions: the channel length is more than $30x$ higher than the channel height. Then, if there are chosen 30 nodes in y direction, it is necessary to set 1000 nodes in the x direction. Hence, the influence of the number of lattice sites is investigated and the solutions are compared at steady state condition. In order to ensure this condition, the temperature is monitored every 1000 time steps for a given target residual, as follows:

$$max_{i,j} \mid T(i,j,t_{n+1000}) - T(i,j,t_n) \mid < 10^{-8} \tag{22}$$

In the case of the three dimensional channel, the sidewall boundaries were considered periodic because the microchannels are considered to be arranged side by side in the heat exchanger. A schematic representation of the three-dimensional microchannel is presented in Fig. 4.

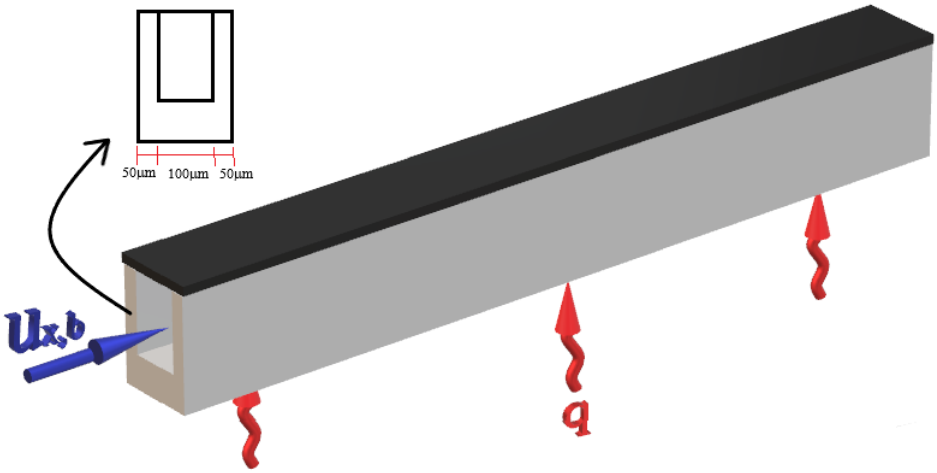

Figure 4. Representation of the thee-dimensional microchannel, where the upper wall is insulated.

It is important to emphasize that the numerical codes were developed in the C language and the MATLAB was used to treat the results data. Otherwise, another important point is that all the simulations were performed in the same computer, in order to guarantee a correct relationship between the measured simulation time.

4. RESULTS AND DISCUSSION

In order to evaluate the accuracy of the results, the simulations are also performed using the commercial CFD software COMSOL®. The global difference between both solutions (by the LBM and the CFD software) is computed by Eq. (23), being $V_{software}$ any value (e.g. temperature variation from the beginning, velocity, pressure, etc) given by the software and V_{LBM} the same quantity, but given by the LBM result.

In Fig. 5, the results of the temperature profiles obtained by the LBM and COMSOL®simulations are presented. The development of the temperature profile in the y direction for different cross sections in x can be seen in the Fig. 6. It can be noticed a good agreement between both results, in which the LBM is capable to capture the correct trends related to the temperature profile. Beside of that, by the Fig. 5, it is possible to see that the principal error of the simulation is related to the temperature field at the solid part of the domain.

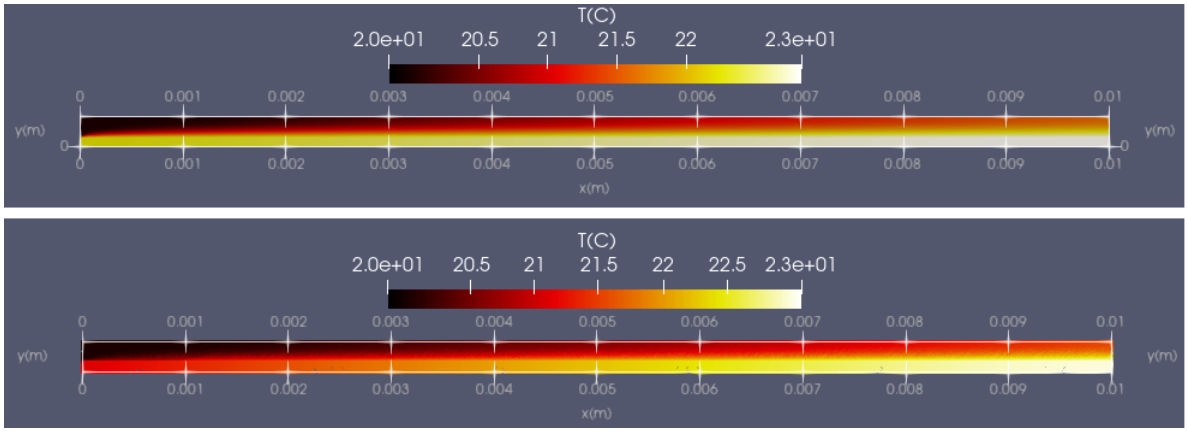

Figure 5. Temperature levels, being (a) the results from Lattice Boltzmann method with $\Delta x = 1.0 \cdot 10^{-5} m$ and $\Delta t = 0.3 \cdot 10^{-6} s$, and (b) the results from COMSOL®.

A possible explanation, as shown in Tab. 1, is related to the accuracy of the method, which decrease with the increase of τ_{gs} when $\tau_{gs} \gg 1$. As α_{solid} is about $600\alpha_{water}$, the relation between τ_g and τ_{gs} maintain a similar order, so, a good value of τ_g results in a higher value of τ_{gs} (higher than 1, in the case), making the results of the simulation at the solid

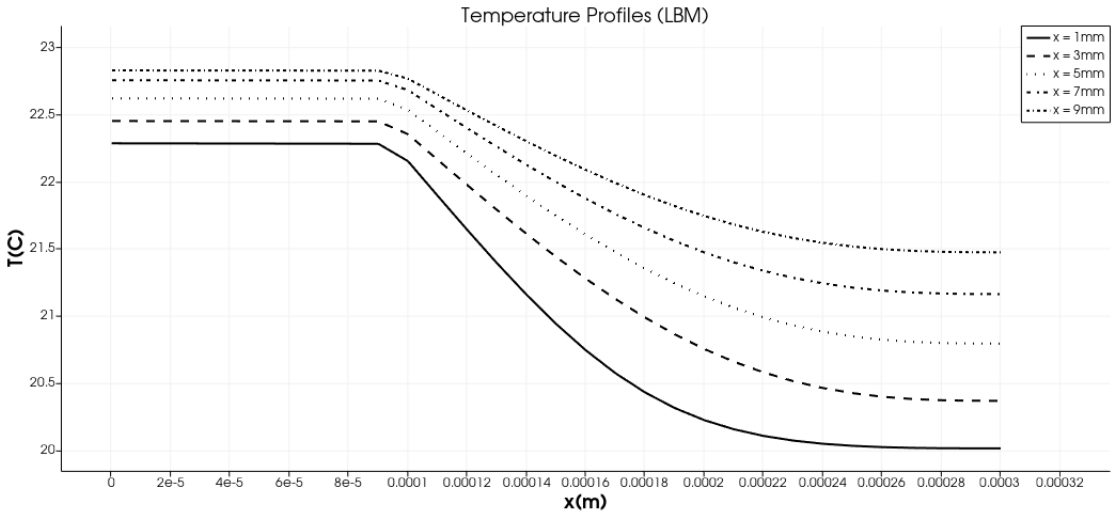

Figure 6. Temperature profiles *versus* height y, gets from Lattice Boltzmann method with $\Delta x = 1.0 \cdot 10^{-5} m$ and $\Delta t = 3.0 \cdot 10^{-6} s$.

region less exact than in the fluid side.

$$GE(\%) = 100 \cdot \frac{\sum_{i=1}^{N} |V_{software} - V_{LBM}|}{\sum_{i=1}^{N} |V_{software}|} \tag{23}$$

Next, the effect of the number of lattices and the relaxation parameter of the solid over the accuracy of the simulations is investigated. This justify the commentaries of the previous paragraph. The results are presented in Tab. 1, as well as the global error computed from each solution, obtained from the LBM and COMSOL®. It can be noticed that with the augmentation of the number of lattices, the space discretization and the simulation time increase, as expected. The time step should be chosen carefully, since, according to Krüger *et al.* (2017), the method becomes unstable as the relaxation parameter is closer to 0.5. This behavior is noted in the referred table, showing an accuracy diminution. In any case, the obtained errors are low.

Table 1. Values of Number of lattices, simulation times, lattice and time step sizes, and the global error when it is compared with a result given by CFD software.

Simulation	Number of lattices	Simulation time (s)	$\Delta x(10^{-5}m)$	$\Delta t(10^{-6}s)$	$GE(\%)$	τ_g	τ_{gs}
1	2500	201.583	2.00	10.000	1.8	0.511	7.480
2	20025	1240.148	1.25	4.000	1.4	0.511	7.648
3	31031	2555.730	1.00	3.000	1.4	0.521	14.460
4	31031	3827.689	1.00	2.000	2.2	0.509	6.084

The results of the 3D simulation are shown in Fig. 7. In order to compare the 2D results with the 3D ones, the results for the middle section are considered. By the analysis of both results, it is evident that the main difference between it are in the temperature profile. In Fig. 5 (more specifically, in Fig. 6), the lower temperature are in the top of the channel, because of the insulated boundary. However, when the lateral fins are considered, there is an extra heat flux in the lateral section, that heats the top of the channel. This is related to the fact that they are made of metal with high thermal conductivity, increasing the temperature at the top of the channel. Thus, it produces a different profile than that seen in the 2D approach, with lower temperatures in the middle of the channel, rather than being in the top. In Fig. 8, the velocity field is presented for the three-dimensional simulation.

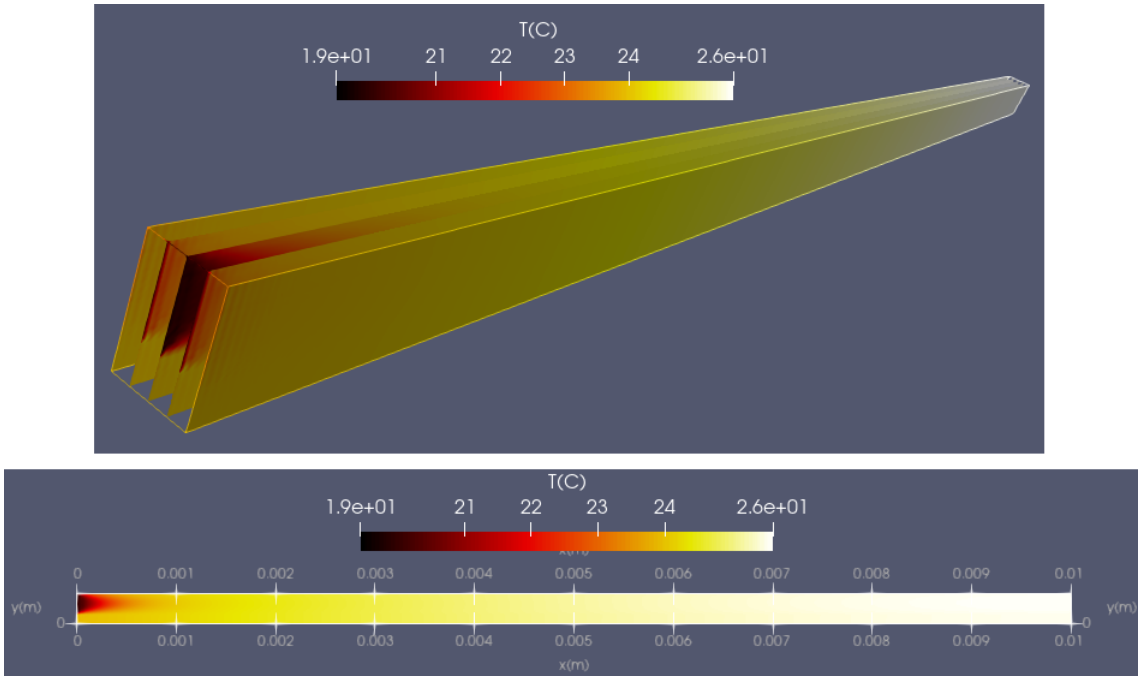

Figure 7. Temperature levels from Lattice Boltzmann method with $\Delta x = 1.0 \cdot 10^{-5} m$ and $\Delta t = 0.3 \cdot 10^{-6} s$, being the second image a longitudinal cut in the middle of the channel.

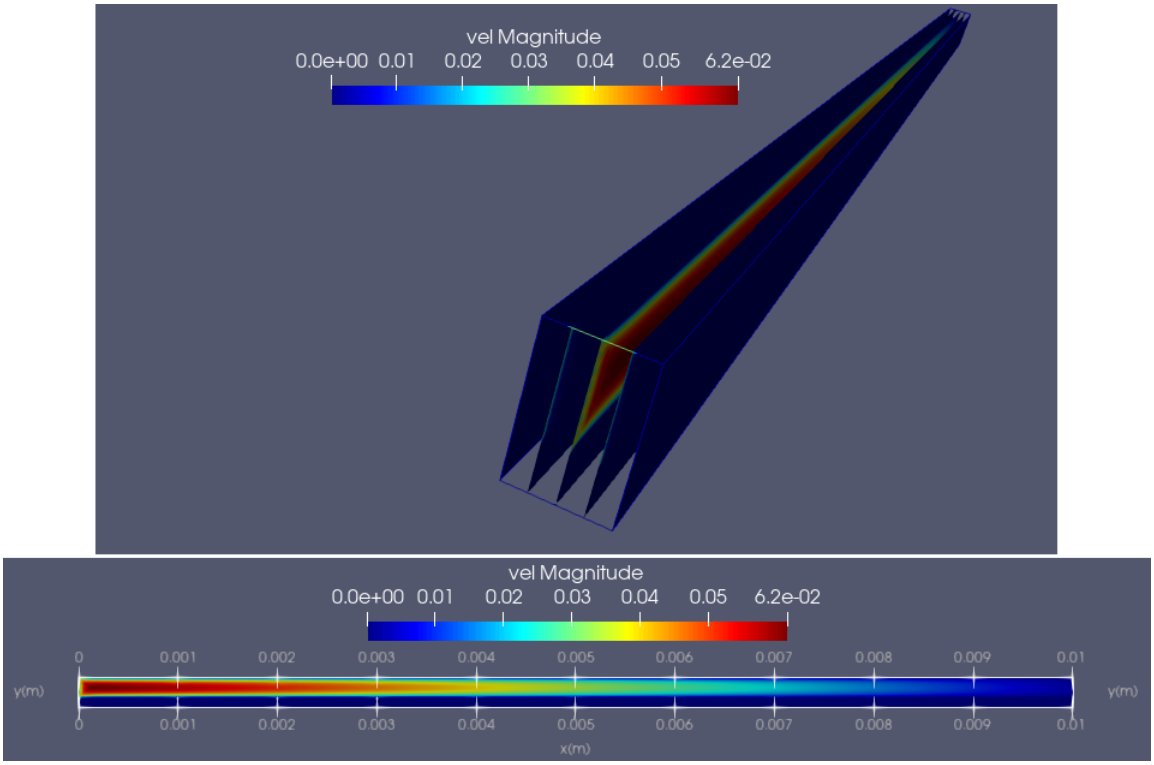

Figure 8. Schematic representation fluid flow and the velocity magnitude (in m/s) for the channel and the middle section of them.

5. CONCLUSIONS

This paper advanced numerical simulations of the conjugate heat transfer in a microchannel. The numerical results were evaluated for two-dimensional and three-dimensional set-ups and compared against numerical results obtained by a commercial software, namely COMSOL®. The influence of the number of lattices and well as space and time discretization over the convergence and the results were performed. For the two-dimensional comparison, the results are in good agreement. Regarding the three-dimensional simulation, it is was noticed that the main difference in the temperature

profile is located at the top region of the microchannel. This is explained by the effect of the lateral fins. As expected, this feature is not captured by the two-dimensional simulation. The performed simulations are a first step for a future work related to boiling heat transfer inside a microchannel using the Lattice Boltzmann Method

6. ACKNOWLEDGMENTS

The authors are grateful for the financial assistance granted by the São Paulo State Research Foundation (FAPESP), processes 2019/21022-9 and 2016/09509-1.

7. REFERENCES

Darzi, A.R., Farhadi, M. and Jourabian, M., 2013. "Lattice boltzmann simulation of heat transfer enhancement during melting by using nanoparticles". *Transactions of Mechanical Engineering*, Vol. 37, No. M1, pp. 23–37.

Guo, Z. and Shu, C., 2013. *Lattice Boltzmann Method and its Application in Engineering*. World Scientific, 3rd edition.

Hardy, J., de Pazzis, O. and Pomeau, Y., 1976. "Molecular dynamics of a classical lattice gas: Transport properties and time correlation functions". *Physical Review A*, Vol. 13, No. 5, pp. 1949–1961.

Hardy, J., Pomeau, Y. and de Pazzis, O., 1973. "Time evolution of a two-dimensional classical lattice system". *Physical Review Letters*, Vol. 31, No. 5, pp. 276–279.

Hecht, M. and Harting, J., 2010. "Implementation of on-site velocity boundary conditions for d3q19 lattice boltzmann simulations". *Journal of Statistical Mechanics: Theory and Experiment*, Vol. 2010, No. 01, p. P01018.

Ho, C., Chang, C., Lin, K. and Lin, C., 2009. "Consistent boundary conditions for 2d and 3d lattice boltzmann simulations". *Computer Modeling in Engineering and Sciences*, Vol. 44, No. 2, pp. 137–155.

Imani, G., Maerefat, M. and Hooman, K., 2012. "Lattice boltzmann simulation of conjugate heat transfer from multiple heated obstacles mounted in a walled parallel plate channel". *Numerical Heat Transfer, Part A: Applications*, Vol. 62, No. 10, pp. 798–821.

Krüger, T., Kusumaatmaja, H., Kuzumin, A., Shardt, O., G and Viggen, E.M., 2017. *The Lattice Boltzmann Method*. Springer, 1st edition.

Mohamad, A.A., 2019. *Lattice Boltzmann Method*. Springer, Calgary, 2nd edition.

Tarokh, A., Mohamad, A.A. and Jiang, L., 2013. "Simulation of conjugate heat transfer using the lattice boltzmann method". *Numerical Heat Transfer, Part A: Applications*, Vol. 63, No. 3, pp. 159–178.

Yu, Y., Wen, Z., Li, Q., Zhou, P. and Yan, H., 2018. "Boiling heat transfer on hydrophilic-hydrophobic mixed surfaces: A 3d lattice boltzmann study". *Applied Thermal Engineering*, Vol. 142, pp. 846–854.

Zhang, T., Shi, B., Guo, Z., Chai, Z. and Lu, J., 2012. "General bounce-back scheme for concentration boundary condition in the lattice-boltzmann method". *Phys. Rev. E*, Vol. 85, No. 2, p. 016701.

8. RESPONSIBILITY NOTICE

The authors are solely responsible for the printed material included in this paper.